

JRC2018-6210

VIBRATION-BASED DEFECT DETECTION FOR FREIGHT RAILCAR TAPERED-ROLLER BEARINGS

Joseph Montalvo

Mechanical Engineering Department
The University of Texas Rio Grande Valley
Edinburg, TX, 78539, USA
joseph.montalvo01@utrgv.edu

Constantine Tarawneh, Ph.D.

Mechanical Engineering Department
The University of Texas Rio Grande Valley
Edinburg, TX, 78539, USA
constantine.tarawneh@utrgv.edu

Arturo A. Fuentes, Ph.D.

Mechanical Engineering Department
The University of Texas Rio Grande Valley
Edinburg, TX, 78539, USA
arturo.fuentes@utrgv.edu

ABSTRACT

The railroad industry currently utilizes two wayside detection systems to monitor the health of freight railcar bearings in service: The Trackside Acoustic Detection System (TADS™) and the wayside Hot-Box Detector (HBD). TADS™ uses wayside microphones to detect and alert the conductor of high risk defects. Many defective bearings may never be detected by TADS™ due to the fact that a high risk defect is considered a spall which spans more than 90% of a bearing's raceway, and there are less than 20 systems in operation throughout the United States and Canada. Much like the TADS™, the HBD is a device that sits on the side of the rail tracks and uses a non-contact infrared sensor to determine the temperature of the train bearings as they roll over the detector. The accuracy and reliability of the temperature readings from this wayside detection system have been concluded to be inconsistent when comparing several laboratory and field studies. The measured temperatures can be significantly different from the actual operating temperature of the bearings due to several factors such as the class of railroad bearing and its position on the axle relative to the position of the wayside detector. Over the last two decades, a number of severely defective bearings were not identified by several wayside detectors, some of which led to costly catastrophic derailments. In response, certain railroads have attempted to optimize the use of the temperature data acquired by the HBDs. However, this latter action has led to a significant increase in the number of non-verified bearings removed from service. In fact, about 40% of the bearings removed from service in the period from 2001 to 2007 were found to have no discernible defects. The

removal of non-verified (defect-free) bearings has resulted in costly delays and inefficiencies.

Driven by the need for more dependable and efficient condition monitoring systems, the University Transportation Center for Railway Safety (UTCRS) research team at the University of Texas Rio Grande Valley (UTRGV) has been developing an advanced onboard condition monitoring system that can accurately and reliably detect the onset of bearing failure. The developed system currently utilizes temperature and vibration signatures to monitor the true condition of a bearing. This system has been validated through rigorous laboratory testing at UTRGV and field testing at the Transportation Technology Center, Inc. (TTCI) in Pueblo, CO. The work presented here provides concrete evidence that the use of vibration signatures of a bearing is a more effective method to assess the bearing condition than monitoring temperature alone. The prototype bearing condition monitoring system is capable of identifying a defective bearing with a defect size of less than 6.45 cm² (1 in²) using the vibration signature, whereas, the temperature profile of that same bearing will indicate a healthy bearing that is operating normally.

INTRODUCTION

The cargo load of each freight railcar is supported by the railcar's suspension components, namely: springs, dampers, axles, wheels, and tapered-roller bearings. Of these components, the bearings are the most susceptible to failure due to the heavy cargo loads at high speeds.

The tapered-roller bearing typically used in freight railcar service has three different fundamental components, namely:

rollers, inner rings (cones), and outer ring (cup). These components, shown in Figure 1, allow for near-frictionless operation under heavy loads and high speeds. However, when one of these components develops a defect, the effectiveness of the near-frictionless rotation is compromised, which may lead to increased frictional heating depending on the size and location of the defect.

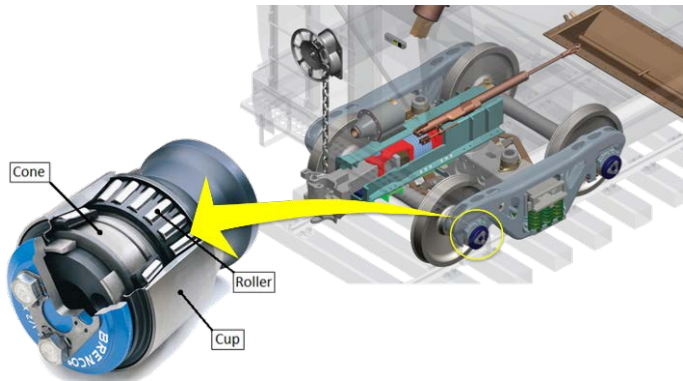


Figure 1. Tapered-Roller Bearing Components [1]

The defects can be categorized into one of three categories: localized defect, distributed defect, or a geometric defect. Two examples of localized defects that include pits, cracks or spalls on a single component of the bearing are illustrated in Figure 2 (left). A distributed defect is when multiple bearing components have localized defects or a single component with multiple defects that are distributed throughout its surface such as a water-etch defect, pictured in Figure 2 (right). Bearings that are out of tolerance due to manufacturing issues or due to geometric inconsistencies are examples of geometric defects.



Figure 2. Example of a localized defect (left) and distributed defect (right)

Bearing Condition Monitoring Systems

The railroad industry currently utilizes two different types of wayside detections systems to monitor the health of the freight car bearings in service: The Trackside Acoustic Detection System (TADS™) and the wayside Hot-Box Detector (HBD).

TADS™ utilizes wayside microphones to detect high-risk defects in bearings and alert the conductor as the train passes by the system. A “growler” is an example of a high risk defect in which spalls occupy more than 90% of the bearing component’s rolling surface. The system is proficient in determining end-of-life bearings. However, there are less than

20 systems in service throughout the United States and Canada, and TADS™ is not capable of identifying defective bearings with small defects [2]. The latter facts suggest that many bearings may spend their entire service life without passing through a TADS™ station, and many other bearings with small defects will go undetected as they pass through TADS™.

Hot-box detectors (HBDs) are the most utilized bearing condition monitoring systems in operation in North America with over 6,000 in use in the United States. They are usually placed 40 km (25 mi) apart, with some positioned 64 km (40 mi) apart on rail lines with less traffic. HBDs use non-contact infrared sensors to measure the temperature radiated from the bearings, wheels, axles, and brakes as they roll over the detector. The HBD will alert the train operator of any bearings running at temperatures greater than 94.4°C (170°F) above ambient conditions. However, bearings operating at temperatures above the average temperature of all bearings on the same side of the train, as detected by multiple HBDs, are said to be “warm trending” [3]. Warm-trended bearings are flagged without triggering an HBD alarm, and are subsequently removed from service for later disassembly and inspection.

Several laboratory and field studies have concluded that the accuracy and reliability of the HBD temperature readings are inconsistent [4]. The measured temperatures can be significantly different from the actual operating temperature of the bearing. The latter can be attributed to several factors such as the class of the railroad bearing and its position on the axle relative to the position of the wayside detector, and environmental conditions that can affect the IR sensor measurements among other possible factors. Inconsistent HBD readings caused 106 severely defective bearings not to be detected by these condition-monitoring systems in the United States and Canada from 2010 to 2016; some of which resulted in costly catastrophic derailments [5]. Attempts by some railroads to remedy the situation by using statistical analysis, run on HBD-acquired data, to set out bearings that run hotter than the average temperature of bearings along one side of the train have resulted in a significant increase in the number of non-verified bearings removed from service. In fact, about 40% of the bearings removed from service in the period from 2001 to 2007 were found to have no discernible defects according to data collected by Amsted Rail. The removal of non-verified bearings has resulted in many costly train stoppages and delays. The study presented here will demonstrate that temperature readings alone are not sufficient for proper characterization of the health of a bearing in service. The vibration signatures of a bearing can be used to identify the onset of bearing defects way before the temperature history can react to those defects. In some cases, bearings with large defects can run at normal operating temperatures for tens of thousands of miles before any abnormality in the operating temperature can be observed. In certain instances, a bearing’s rolling raceway may deteriorate rapidly and cause severe roller misalignment. The misaligned rollers generate excessive frictional heating, which can weaken an axle within 60 to 135 seconds, and may lead to a catastrophic derailment depending on the traveling speed of the

train and the load it is carrying [6]. The latter implies that catastrophic failure can occur between two consecutive HBDs, which highlights the need for an onboard monitoring system.

EXPERIMENTAL SETUP & PROCEDURES

The University Transportation Center for Railway Safety (UTCRS) dynamic bearing testers shown in Figure 3 were used to perform all relevant experiments for this study. Both test rigs can accommodate Class F (6 1/2" x 12") and Class K (6 1/2" x 9") tapered-roller bearings. A fully loaded railcar applies a load of 153 kN (34.4 kip) per bearing, and each tester is equipped with a hydraulic cylinder that allows each test bearing to be loaded up to 175% of a fully-loaded railcar. The data provided in this paper were collected utilizing three loading conditions; namely, 17% of full load, which represents an empty railcar, 100% of full load, which corresponds to a fully loaded railcar, and 110% of full load, which simulates an overloaded railcar. The test rigs are equipped with a 22 kW (30 hp) variable speed motor which allows the bearings to be tested at the different velocities listed in Table 1. The bearings are air-cooled utilizing two industrial size fans that produce an air stream traveling at an average speed of 5 m/s (11.2 mph).



Figure 3. Single Bearing Test Rig (left), Four-Bearing Test Rig (Right)

Table 1. Typical speeds used to perform the experiments in this study.

Axle Speed [RPM]	Track Speed [km/h] / [mph]
280	48 / 30
327	56 / 35
373	64 / 40
420	72 / 45
467	80 / 50
498	85 / 53
514	89 / 55
560	97 / 60
618	106 / 66
699	121 / 75
799	137 / 85

The Single Bearing Test Rig (SBT) shown in Figure 3 (left) accommodates a single railroad tapered-roller bearing in a cantilever setup, which closely mimics the bearing loading conditions on a freight railcar. A bearing adapter was specially machined to accept four 70g accelerometers (placed in the Smart Adapter (SA) and Mote (M) locations at the inboard and outboard sides of the bearing), one 500g accelerometer (placed in the Radial (R) location on the outboard side), and four K-type bayonet thermocouples (two inboard and two outboard). In addition to the four thermocouples affixed to the bearing adapter, there are seven K-type thermocouples placed equidistantly around the circumference of the bearing outer ring (cup), and held in place tightly via a hose clamp.

The Four-Bearing Test Rig (4BT) shown in Figure 3 (right) accommodates either four Class F or Class K bearings pressed onto a test axle. The instrumentation setup for the 4BT is given in Figure 4. In order to replicate field service conditions, only data collected from the middle two bearings (B2 and B3) were used for this study since they are both top-loaded. Thus, the middle two bearing adapters were machined to accept two 70g accelerometers (placed in the outboard SA and M locations), one 500g accelerometer (placed in the outboard R location), two K-type bayonet thermocouples, and one regular K-type thermocouple aligned with the two bayonet thermocouples and placed midway along the bearing cup width, held tightly by a hose clamp. Figure 5 shows the Smart Adapter (SA), Mote (M), and Radial (R) locations of the accelerometers on the modified bearing adapter.

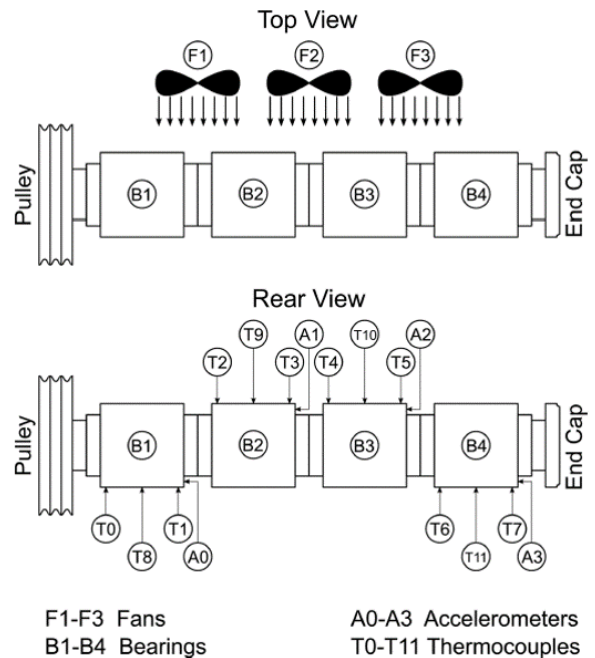


Figure 4. Top and rear views of 4BT including sensor locations

A National Instruments (NI) PXIe-1062Q data acquisition system (DAQ) programmed using LabVIEW™ was utilized to record and collect all the data for this study. A NI TB-2627 card

was used to collect the thermocouple temperature data at a sampling rate of 128 Hz for half a second, in twenty second intervals. An 8-channel NI PXI-4472B card was used to record and collect the accelerometer data for this study. Accelerometer data was recorded and collected at a sampling rate of 5,120 Hz for sixteen seconds, in ten-minute intervals. The root-mean-square of the accelerometer data was then used for the analysis.

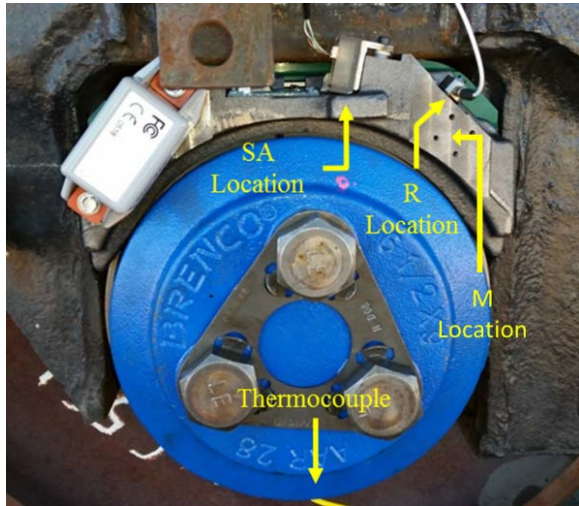


Figure 5. Modified bearing adapter showing sensor locations

Field Test

In 2015, the UTCRS research team, in collaboration with Amsted Rail Engineers, conducted a proof of concept field test at the Transportation Technology Center, Inc. (TTCI) in Pueblo, Colorado. The primary objective of the field test is to validate the accuracy and reliability of the onboard accelerometer-based condition monitoring system in detecting defective bearings. A locomotive towing a business car and an instrumented freight railcar (empty one day and fully loaded the second day) along different TTCI tracks at speeds ranging from 48 to 105 km/h (30 to 65 mph) provided the field-test data for this study. The data acquisition system was set up in the business car. Figure 6 is a picture of the business car and the freight railcar as the UTCRS research team was completing the instrumentation in preparation for the field test at TTCI.



Figure 6. A picture of the business car and the freight railcar being instrumented for the field test at TTCI

It is important to note that this field test was implemented as a blind test; *i.e.*, the UTCRS researcher in charge of analyzing the data did not know the type and location of the four defective bearings within the freight railcar. Out of the eight railroad bearings on the instrumented freight railcar, four were defect-free (healthy), two contained outer ring (cup) defects (spalls), and two had inner ring (cone) defects (spalls). Figure 7 provides the locations of the healthy and defective bearings on the instrumented freight railcar, and Figure 5 shows the sensors used in this field test along with their location on the bearing/adapter assembly.

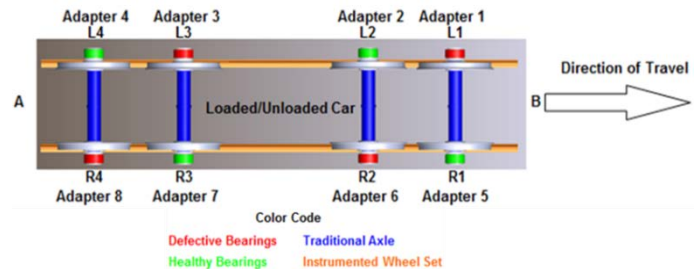


Figure 7. Test Railcar Setup at TTCI

The field test utilized two different TTCI tracks in order to evaluate the difference in results when the train travels over a smooth versus a rough track. One 70g and one 500g accelerometer were mounted on each bearing adapter at the SA and R locations (see Figure 5), respectively. Note that the 70g accelerometer is mounted on a special circuit board, and the signal produced by this accelerometer passes through specially designed electronic signal conditioning circuitry to filter out any external noise interference prior to being connected to the NI 9215 card. The special circuit board and the signal conditioning circuitry were designed and fabricated by the UTCRS research team as part of the onboard vibration-based bearing health monitoring system development efforts. The 500g accelerometer that is mounted on the adapter at the Radial (R) location is commercially available, has built-in signal conditioning, and plugs directly to the NI 9234 card connected to the DAQ system. In the field test, temperature data was collected at a sampling rate of 128 Hz for half a second, in fifteen second intervals, whereas, the accelerometer data were collected continuously at a rate of 5,556 Hz. All instrumentation was powered by the locomotive. The final version of the prototype onboard sensor will be wireless and battery-powered.

LABORATORY RESULTS

A study that compared the temperature profiles for defect-free (healthy) bearings to those of bearings with defective inner (cone) and outer (cup) rings was carried out by the UTCRS research team in 2016 [7]. The study demonstrated that the operating temperature was not a good predictor of bearing health since bearings with defective inner and outer rings operated at temperatures that are comparable to those of healthy

bearings [7]. The latter study resulted in the development of a correlation for the average operating temperatures for healthy (defect-free) bearings at several speeds for empty and fully-loaded freight railcars. This correlation is used in this current study as a reference for normal operating bearing temperatures at the specified speed and load.

Experiment 203

In Experiment 203, a defective bearing with an outer ring (cup) spall on the outboard raceway, approximately 0.865 cm² (0.134 in²) in initial size, was run on the four-bearing tester (4BT). The bearing with the initial defect shown in Figure 8 (left) was placed in the B3 position on the 4BT (see Figure 4). The spall propagated throughout the course of the experiment and grew in size to 9.50 cm² (1.47 in²), as depicted in Figure 8 (right). For direct comparison, the bearing placed in the B2 position right next to the defective bearing (B3) is a control (defect-free) bearing that is run at the same exact load and speed operating conditions.



Figure 8. Starting cup spall for Bearing 3 (left); ending cup spall for Bearing 3

The bearings were initially run at a speed of 64 km/h (40 mph) and a full load (153 kN or 34.4 kip per bearing) in order to allow the grease to break in, after which, the test conditions were changed to 137 km/h (85 mph) and 110% of full load. The vibration and temperature profiles for the defective versus the control bearing are displayed in Figure 9. Looking at the temperature histories for both bearings, two observations can be made; first, both bearings seem to be running at or below the average operating temperature correlation for control bearings depicted by the solid red line, with the exceptions being at the initial break in period and the settling periods following abrupt changes in operating conditions; second, the healthy bearing is running hotter than the defective bearing throughout the experiment, which is counterintuitive. Table 2 provides a summary of the results depicted in Figure 9.

Examining the vibration signatures of the healthy versus the defective bearing shown in Figure 9, and looking at the

average root-mean-square (RMS) values of the accelerations summarized in Table 2, it is evident that the defective bearing (Bearing 3) has a higher vibration signature than the healthy bearing (Bearing 2). As stated earlier, the spall within the defective bearing propagated during the experiment, which resulted in a significant increase in the vibration levels of that bearing as exhibited by the RMS values listed in Table 2. Previous testing performed has revealed that as the defect size increases, the vibration levels of the bearing increase as well. This increase is attributed to small metal pieces surrounding the spall region that break off and affect the rotational behavior of the bearing rolling elements. As the bearing continues to operate, the metal debris circulates throughout the bearing and gets crushed by the rollers. When that happens, the vibration levels of the bearing decrease as the metal shards shrink in size. This cycle will repeat itself every time the spall deteriorates introducing more metal debris into the bearing rolling raceways. This behavior is captured through the vibration oscillations of Bearing 3 (defective) seen in Figure 9. Both accelerometers on Bearing 3 (SA and M locations) exhibit this behavior after the change in the load and speed operating conditions. However, Bearing 2 (healthy) does not exhibit any oscillations, and maintains near constant vibration levels at each operating condition.

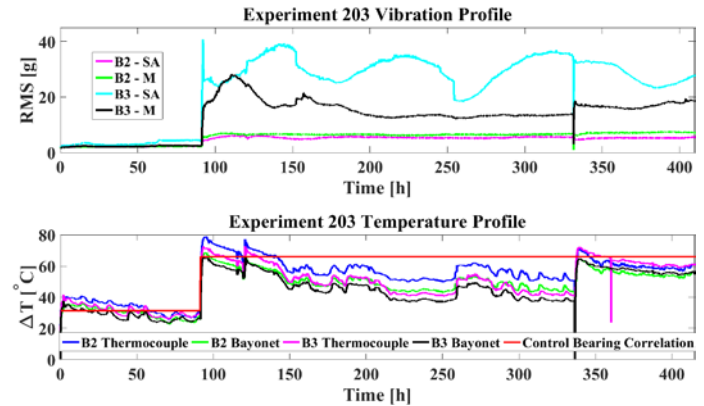


Figure 9. Vibration and temperature profiles for Experiment 203

Table 2. Average values for Experiment 203 for Bearing 2 and Bearing 3 (Average ambient temperature was 20°C or 68°F)

Bearing 2 (Healthy)				
Track Speed [km/h]/[mph]	Load [%]	ΔT [°C / °F]	Control ΔT [°C / °F]	RMS [g]
64/40	100	31.7/57.1	31.4/56.5	2.1
137/85	110	55.5/99.9	66.0/118.8	6.0
Bearing 3 (Defective)				
Track Speed [km/h]/[mph]	Load [%]	ΔT [°C / °F]	Control ΔT [°C / °F]	RMS [g]
64/40	100	29.7/53.5	31.4/56.5	2.8
137/85	110	51.5/92.7	66.0/118.8	22.9

Based on the results presented for Experiment 203, relying solely on the temperature histories of both bearings, one might deduce that they are defect-free (healthy) bearings. In fact, the average operating temperature of the defective bearing as indicated by the regular and bayonet thermocouples is lower than that of the healthy bearing. The latter behavior has been witnessed in several experiments performed using a similar setup with one defective bearing running alongside a healthy bearing, which validates the argument that the operating temperature alone is not a good indicator of the presence of defects within a bearing. On the other hand, looking at the vibration data, a healthy bearing running at 137 km/h (85 mph) with a 110% load condition has a maximum average acceleration of 6g; so, the 22.9g average acceleration exhibited by Bearing 3 clearly indicates a defective bearing regardless of its operating temperature. Bearing 2 of Experiment 203 will be referred to as the control bearing hereafter.

Experiment 204

Two defective bearings were used in Experiment 204: Bearing 2 has a spalled cone (inner ring), whereas, Bearing 3 has a pitted cone raceway. Bearing 2 had a starting spall size of approximately 2.85 cm² (0.441 in²), and an ending spall size of 5.04 cm² (0.781 in²). The pits on Bearing 3 did not grow. Figure 10 and Figure 11 depict the starting and ending defect size for Bearing 2 and Bearing 3, respectively.



Figure 10. Starting cone spall for Bearing 2 (left); ending cone spall for Bearing 2 (right)



Figure 11. Starting pitted cone raceway for Bearing 3 (left); ending pitted cone raceway for Bearing 3 (right)

Again, the results of Experiment 204 demonstrate that the bearing operating temperature alone is not adequate to identify defects in bearings. Looking at Figure 12 and the results summarized on Table 3, it can be observed that both defective bearings operated at or below the average operating temperature of the control (defect-free) bearing, with Bearing 2 running slightly hotter than Bearing 3. However, when examining the average RMS values for both bearings, it is clear that the vibration levels of Bearing 2 (the one with the spall) are higher than those for the control bearing at all loading and speed conditions. As for Bearing 3 (the one with the cone raceway pits), the vibration levels begin to exceed those of the control bearing at the highest load and speed conditions, which is not surprising given that these pits are very minimal in size. As stated earlier, the spall of Bearing 2 propagated during the experiment. By observing the vibration history of Bearing 2, it appears that the spall is still approximately 2.85 cm² (0.441 in²) in size during the lower speed and load conditions. The latter implies that the devised vibration-based condition monitoring system is capable of reliably detecting defects less than 3.22 cm² (0.500 in²) in size.

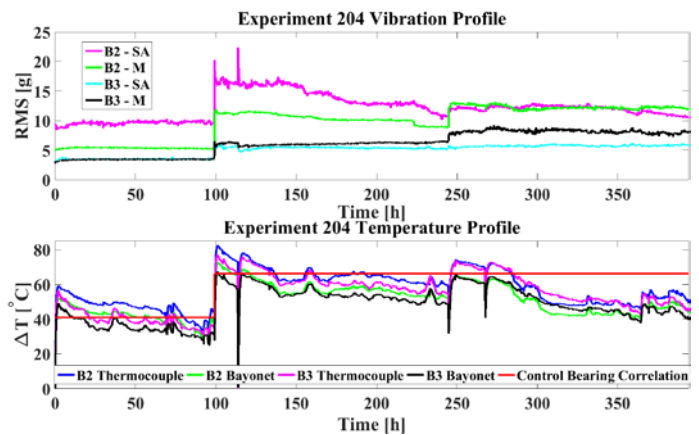


Figure 12. Vibration and temperature profiles for Experiment 204

Table 3. Average values for Experiment 204 for Bearing 2 and Bearing 3 (Average ambient temperature was 20°C or 68°F)

Bearing 2 (Large Spall Across Cone Raceway)				
Track Speed [km/h]/[mph]	Load [%]	ΔT [°C / °F]	Control ΔT [°C / °F]	RMS [g]
85/53	100	44.0/79.2	41.0/73.8	6.5
137/85	110	57.5/103.5	66.0/118.8	12.2
Bearing 3 (Pitted Cone Raceway)				
Track Speed [km/h]/[mph]	Load [%]	ΔT [°C / °F]	Control ΔT [°C / °F]	RMS [g]
85/53	100	37.7/67.9	41.0/73.8	3.4
137/85	110	56.1/100.1	66.0/118.8	6.3

Note that the increase in the vibration levels as the spall propagated was masked by the change in speed and load conditions. The ensuing decrease in the vibration levels of Bearing 2 is the result of the small metal shards that broke off from the spall shrinking in size and being pushed out of the way by the rollers. Finally, it is important to point out that the increase in the vibration levels of Bearing 3 at around 245 hours into the test, as indicated by the accelerometer in the mote (M) location, mimics the increase exhibited by the mote location accelerometer of Bearing 2, and is the result of the cross-talk between the two bearings that are next to each other.

Experiment 206

Experiment 206 was carried out on the single bearing tester (SBT) and was intended to examine a severely defective inner ring (cone) with large size spalls, as pictured in Figure 13. The test bearing originally contained a defective cone with six spalls, as shown in Figure 13 (left). After the experiment ended, it was noticed, upon teardown and disassembly, that three of the spalls had combined forming a large rough patch that covered a significant area of the cone, as can be seen in Figure 13 (right). Table 4 lists all the spall sizes pre- and post-testing. The test bearing was run at three different speeds and two loading conditions, 17% load (empty railcar), and 100% load (full railcar). By the end of the experiment, the cone raceway had degraded to the point where the motor was not able to rotate the axle due to roller misalignments in the defective bearing.

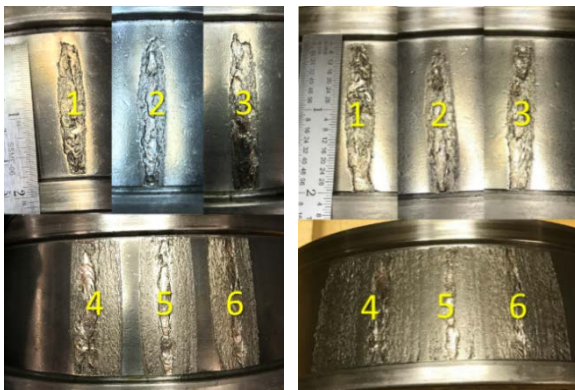


Figure 13. Starting cone spalls for Experiment 206 (left); ending cone spalls for Experiment 206 (right)

Table 4. Size comparison of pre- and post-experiment inner ring (cone) spalls for the test bearing of Experiment 206

Spall #	Pre-Testing Spall Size [cm ²] / [in ²]	Post-Testing Spall Size [cm ²] / [in ²]
1	4.071 / 0.631	4.516 / 0.700
2	3.374 / 0.523	3.929 / 0.609
3	3.555 / 0.551	4.258 / 0.660
4	8.871 / 1.375	40.77 / 6.320
5	9.374 / 1.453	
6	9.252 / 1.434	
Total	38.50 / 5.967	53.48 / 8.289

Looking at Figure 14 and Table 5, it is evident that the test bearing vibration levels far exceed those of a control (healthy) bearing for similar loading conditions. At 64 km/h (40 mph) and 100% load, the test bearing RMS value is about five times that of a control bearing while still operating at a temperature that is only 3°C (5°F) higher than the operating temperature of the control bearing correlation. In fact, the highest average operating temperature of this test bearing is only 5.3°C (9.5°F) greater than the control bearing correlation. None of the operating temperatures for this defective bearing are high enough to trigger the HBD alarm threshold of 94.4°C (170°F) above ambient conditions set by the Association of American Railroads (AAR). The latter is a cause for concern given the severity of the defects within this bearing and the fact that the test rig was having difficulties rotating the axle due to the high roller misalignments causing the bearing to lock up. A bearing with a similar defective cone in field service would have probably seized under similar operating conditions. The train’s momentum would cause the rollers to heat up excessively and melt the bearing onto the axle, which may lead to a catastrophic derailment depending on the traveling speed of the train and the load it is carrying.

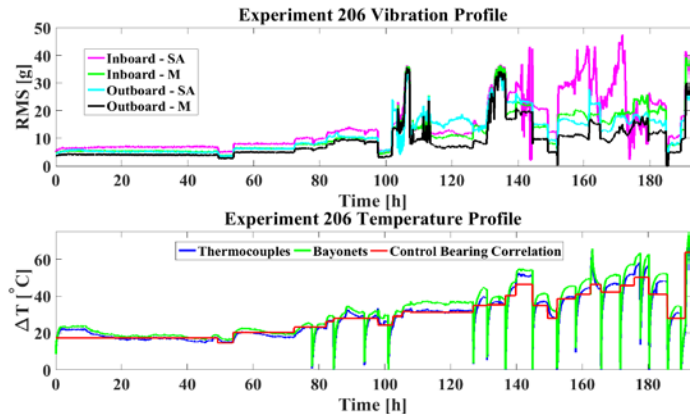


Figure 14. Vibration and temperature profiles for bearing 1 for Experiment 206

Table 5. Average values for test bearing for Experiment 206 (Average ambient temperature was 20°C or 68°F)

Test Bearing (Six Large Cone Spalls)				
Track Speed [km/h]/[mph]	Load [%]	ΔT [°C / °F]	Control ΔT [°C / °F]	RMS [g]
48/30	17	16.1/29.0	14.6/26.2	3.8
64/40	17	19.8/35.6	20.3/36.6	5.3
137/85	17	51.6/92.9	46.3/83.3	22.3
48/30	100	26.3/47.3	24.2/43.6	4.8
64/40	100	34.2/61.6	31.4/56.5	10.2
137/85	100	65.4/117.7	63.7/114.6	37.3

FIELD TEST RESULTS

UTCRS researchers along with Amsted Rail engineers instrumented a railcar at TTCI in Pueblo, CO, with accelerometers and thermocouples, as depicted in Figure 5. As described earlier, this test was intended to be a blind test in order to validate the developed vibration-based bearing condition monitoring technology. Hence, four defective and four healthy bearings were strategically positioned throughout the railcar. For brevity, this section will focus on the four bearings located at the front half of the railcar during the first day of field testing. Bearing L1 had a defective cone with a total spall area of 14.2 cm² (2.2 in²), as shown in Figure 15. Bearing R2 had a defective outer ring (cup) with a total spall area of 34.2 cm² (5.3 in²), as pictured in Figure 16. The railcar operated at speeds of 48 km/h (30 mph), 80 km/h (50 mph), and 89 km/h (55 mph) with a full load (153 kN or 34.4 kip per bearing). The average ambient temperature during this test was 17.5°C (63.5°F). Figure 17 along with Table 6 and Table 7 summarize the most relevant results of this test.



Figure 15. Photographs of Bearing L1 inner ring (cone) defect



Figure 16. Photograph of Bearing R2 outer ring (cup) defect

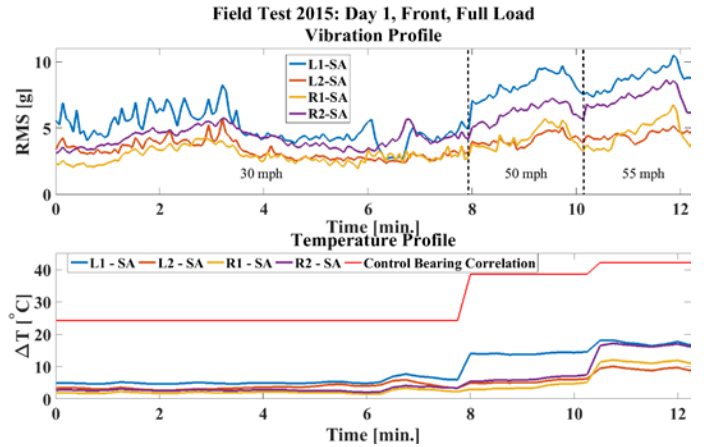


Figure 17. Vibration and temperature profiles for defective and healthy bearings located at the front of a fully loaded railcar (refer to Figure 7)

Table 6. Summary of Bearings L1 and L2 temperature and vibration profiles

Bearing L1 (Cone Spall)				
Track Speed [km/h]/[mph]	Load [%]	ΔT [°C / °F]	Control ΔT [°C / °F]	RMS [g]
48/30	100	5.2/9.4	24.2/43.6	5.0
80/50	100	14.1/25.3	38.6/69.4	8.2
89/55	100	17.2/31.0	42.2/75.9	8.8
Bearing L2 (Healthy)				
Track Speed [km/h]/[mph]	Load [%]	ΔT [°C / °F]	Control ΔT [°C / °F]	RMS [g]
48/30	100	3.7/6.6	24.2/43.6	3.3
80/50	100	5.4/9.7	38.6/69.4	4.1
89/55	100	9.3/16.8	42.2/75.9	4.5

Table 7. Summary of Bearings R1 and R2 temperature and vibration profiles

Bearing R1 (Healthy)				
Track Speed [km/h]/[mph]	Load [%]	ΔT [°C / °F]	Control ΔT [°C / °F]	RMS [g]
48/30	100	2.1/3.7	24.2/43.6	2.9
80/50	100	3.8/6.8	38.6/69.4	4.3
89/55	100	11.5/20.6	42.2/75.9	4.6
Bearing R2 (Cup Spall)				
Track Speed [km/h]/[mph]	Load [%]	ΔT [°C / °F]	Control ΔT [°C / °F]	RMS [g]
48/30	100	2.8/5.1	24.2/43.6	4.2
80/50	100	6.3/11.3	38.6/69.4	6.2
89/55	100	16.5/29.8	42.2/75.9	7.3

According to Figure 17, Table 6, and Table 7, the defective Bearings L1 and R2 have vibration levels that are, on average, 50% higher than those for the healthy Bearings L2 and R1. When comparing these four bearings to the control bearing values established in Table 2, it is evident that Bearings L1 and R2 operating at 100% load with speeds of 89 km/h (55 mph) and lower exhibit vibration levels that are 33% higher than those of the control bearing operating at a speed of 137 km/h (85 mph) with an overload of 110%. In contrast, Bearings L2 and R1 have vibration levels that fall in-line with the control bearing. Examining the temperature histories of the four bearings, it can be observed that the defective Bearings L1 and R2 are running at higher operating temperatures than those of the healthy Bearings L2 and R1, but the operating temperatures of all four bearings are well below the average operating temperatures given by the control bearing correlation. Moreover, the operating temperatures of the two defective bearings are well below the HBD alarm threshold. Similar trends are shown by the back four bearings for this test day, and for the second day field tests performed under different loading conditions. These results demonstrate the effectiveness of the devised vibration-based bearing condition monitoring system.

CONCLUSIONS

Current wayside condition monitoring systems are reactive in nature in that they normally detect defective bearings towards the end of their lives. This does not allow for appropriate maintenance cycles throughout the time the bearing is defective. Hot-box detectors (HBDs) rely on temperature measurements along and are, therefore, not very effective at identifying bearings with defects at early stages of development since the operating temperature of these bearings is usually within the operating temperatures of healthy (defect-free) bearings. Not only have HBDs failed to identify defective bearings that ultimately led to derailments, almost 40% of bearings removed from service due to warm temperature trending as flagged by HBDs turned out to be defect-free bearings. Hence, temperature measurements alone are not a reliable metric for determining bearing health.

TADS™ are not a good alternative to HBDs due to the low number of units in service as well as the fact that they are programmed to flag “growlers” (*i.e.*, bearings containing a component with a defect that covers 90% of the contact raceway surface area), and the train must be stopped immediately to get the bearing replaced. Had the defective bearings been identified at an earlier stage, proactive maintenance could have been scheduled, which would have avoided the costly train stoppages and service interruptions.

Since the current wayside detection systems are inefficient, a new onboard vibration-based bearing condition monitoring system has been developed at the UTCRS laboratories, and field-tested and validated at TTCI. The new onboard condition monitoring system utilizes accelerometers to track the health of railroad bearings in service through their vibration signatures. This new system can accurately and reliably identify bearing

defects as small as 2.85 cm² (0.441 in²) and track the defects as they deteriorate. The latter allows railroads to implement proactive maintenance schedules and avoid costly and unnecessary train delays and/or stoppages. Additionally, removing bearings from service before their defects become catastrophic will prevent severe damages to rail infrastructure resulting from railcar derailments.

Based on the results of this study, it will be possible to identify bearing vibration thresholds to determine the onset of defect formation and track its deterioration through the vibration levels within the bearing. Once a bearing is determined to be defective, efforts will be placed into identifying the defect location and quantifying its size from the vibration signature. This data will then be used in conjunction with other research carried out at the UTCRS to estimate the remaining service life of a defective bearing so that proactive and cost-effective maintenance schedules can be implemented.

ACKNOWLEDGMENTS

This study was made possible by funding provided by The University Transportation Center for Railway Safety (UTCRS), through a USDOT Grant No. DTRT 13-G-UTC59. The collaboration and assistance of Amsted Rail, a private rail industry, was instrumental to the success of this study.

REFERENCES

- [1] “Freight Car Components.” *Freight Car Components Amsted Rail*. Web. <https://www.amstedrail.com/products-services/freight-car-components>
- [2] DataTraks Secures Contract to Manage TADS for TTCI built in colorado. Web. <https://www.builtincolorado.com/blog/datatraks-secures-contract-manage-trackside-acoustic-detection-system-tads>
- [3] H. Wang, T.F. Conry, C. Cusano, “Effects of cone/axle rubbing due to roller bearing seizure on the thermomechanical behavior of a railroad Axle,” *Journal of Tribology*, Vol. 118, pp. 311-319, 1996.
- [4] Mealer, A., Tarawneh, C., Crown, S., “Radiative Heat Transfer Analysis of Railroad Bearings for Wayside Hot-box Detector Optimization,” *Proceedings of the 2017 Joint Rail Conference*, Philadelphia, PA, April 4-7, 2017.
- [5] 2.09 - Train Accidents and Rates | Federal Railroad Administration, Office of Safety Analysis. Web. safetydata.fra.dot.gov/OfficeofSafety/publicsite/query/TrainAccidentsFYCYWithRates.aspx.
- [6] S. Karunakaran, T.W. Snyder, “Bearing temperature performance in freight cars,” *Proceedings Bearing Research Symposium, ASME RTD Fall Conference*, Chicago, IL, September 11-12, 2007.
- [7] Tarawneh, C., Sotelo, L., Villarreal, A. A., De Los Santos, N., Lechtenberg, R. L., Jones, R., “Temperature Profiles of Railroad Tapered Roller Bearings with Defective Inner and Outer Rings,” *Proceedings of the 2016 Joint Rail Conference*, Columbia, SC, April 12-15, 2016.